Electronic Supplementary Information

A fully automated primary neuron purification system using continuous centrifugal microfluidics

Aseer Intisar,[a] Seung Joon Lee,[b] Yu-Gyeong Kim,[b] Woon-Hae Kim,[a] Hyun Young Shin,[a] Min Young Kim,[a] Jong Man Kim,[b] Jungmin Lee,[b] Yun Jeoung Mo,[c] Yu Seon Kim,[c] Seung-Hoon Kim,[b] Yun-Il Lee[c] and Minseok S. Kim*[abde]

[a] Department of New Biology, DGIST, Daegu 42988, Republic of Korea

[b] CTCELLS Corp., Daegu 42988, Republic of Korea

[c] Well Aging Research Center, DGIST, Daegu 42988, Republic of Korea

[d] Translational Responsive Medicine Center (TRMC), DGIST, Daegu 42988, Republic of Korea

[e] New Biology Research Center (NBRC), DGIST, Daegu 42988, Republic of Korea

* Corresponding author. Email: kms@dgist.ac.kr

COMSOL Multiphysics simulation of force exerted on the fluid

In order to increase the depletion efficiency of non-neuronal cells captured by immunomagnetic microbeads in the purification chamber, a unidirectional magnetic force induced by Halbach array magnets was applied together with centrifugal force. COMSOL Multiphysics 5.3a was used to simulate the total force exerted on the fluid during the centrifugal microfluidic purification process. Laminar flow and magnetic field modules were used to simulate centrifugal and magnetic forces, respectively. Simulation showed that, the magnetic flux induced by the magnets (Halbach array) enhanced the total force exerted on the fluid. Figure S1A demonstrates the existing (top image) and non-existing (bottom image) magnetic force due to the presence and absence of the magnets, respectively, beneath the purification chamber. At zero RPM, the magnetic force exerted on the fluid is shown in Figure S1B. While the centrifugal force exerted on the fluid at a rotation rate of 50 RPM with no magnets can be seen in Figure S1C. At low centrifugal force (50 RPM), magnetic force induced by the magnets presented most of the total force exerted on the fluid as shown in Figure S1 D and E. As the rotation rate (RPM) increased (500 RPM), centrifugal and magnetic forces exerted on the fluid are almost equal as seen in Figure S1 F and G. Furthermore, at higher rotation rate, such as 1,500 RPM, centrifugal force exerted on the fluid is more dominant than the magnetic force induced by the magnets as shown in Figures S1 H and I. These simulation results suggest that non-neural cells captured by immunomagnetic beads can be depleted more effectively by the combined magnetic and centrifugal forces at the initial acceleration stage.

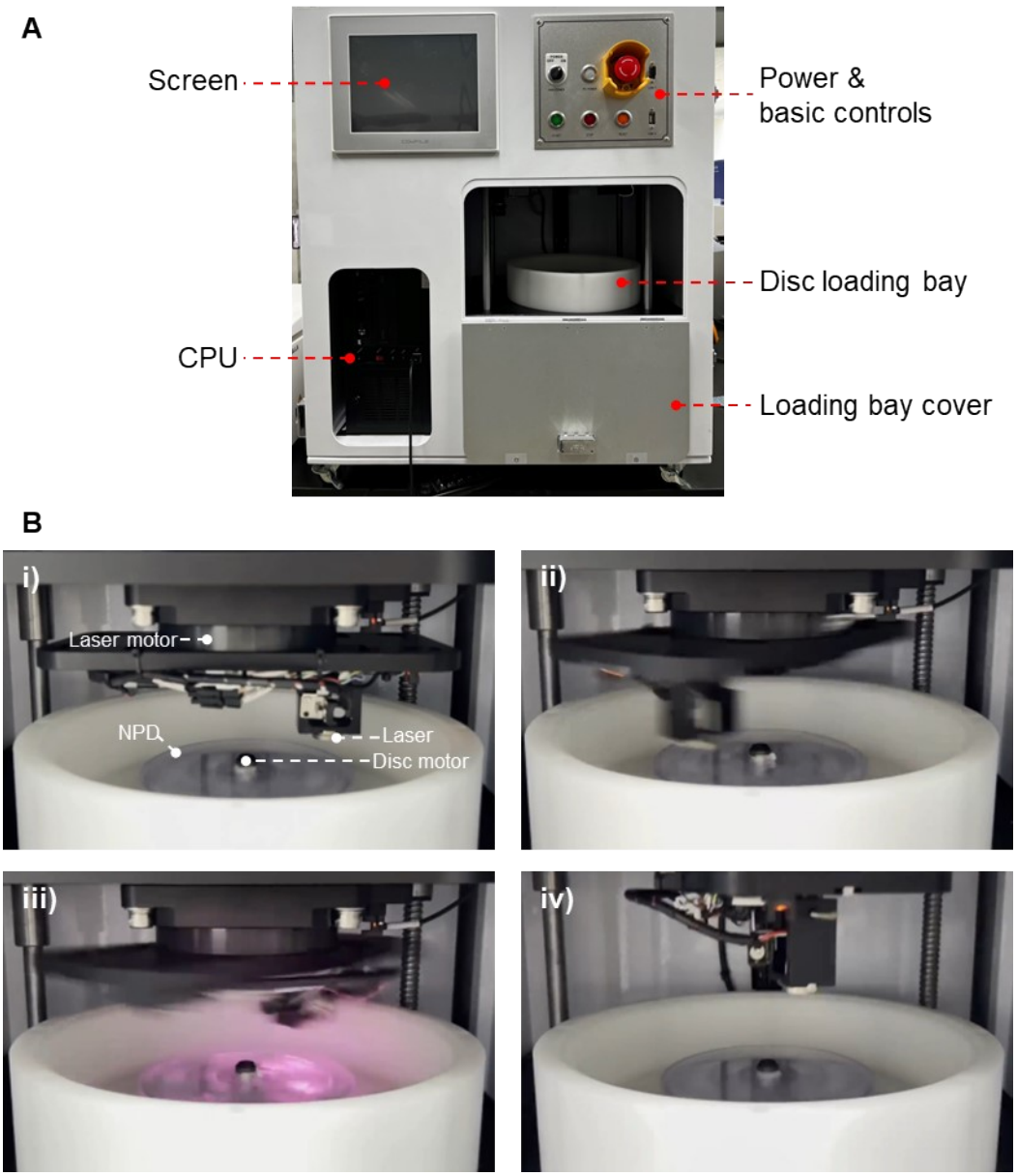

Fig. S1 (A) The instrumentation used for centrifugation and disc-laser synchronization. The disc motor is situated inside the disc loading bay, and contains a slot for placing the disc. The loading bay cover is closed during the operation of the instrument. The screen displays the parameters set for individual steps of the purification process. (B) Images showing sequential steps during valve opening via laser exposure using the continuous centrifugal microfluidics (CCM) technique. (i) The laser unit is lowered closer to the disc, and the disc decelerates to 300 RPM. (ii) The angular speed and phase of rotation of the disc and laser are synchronized. (iii) Laser exposure to open valve. (iv) After laser exposure, the laser unit is raised up and the disc accelerates to the desired rotation speed.

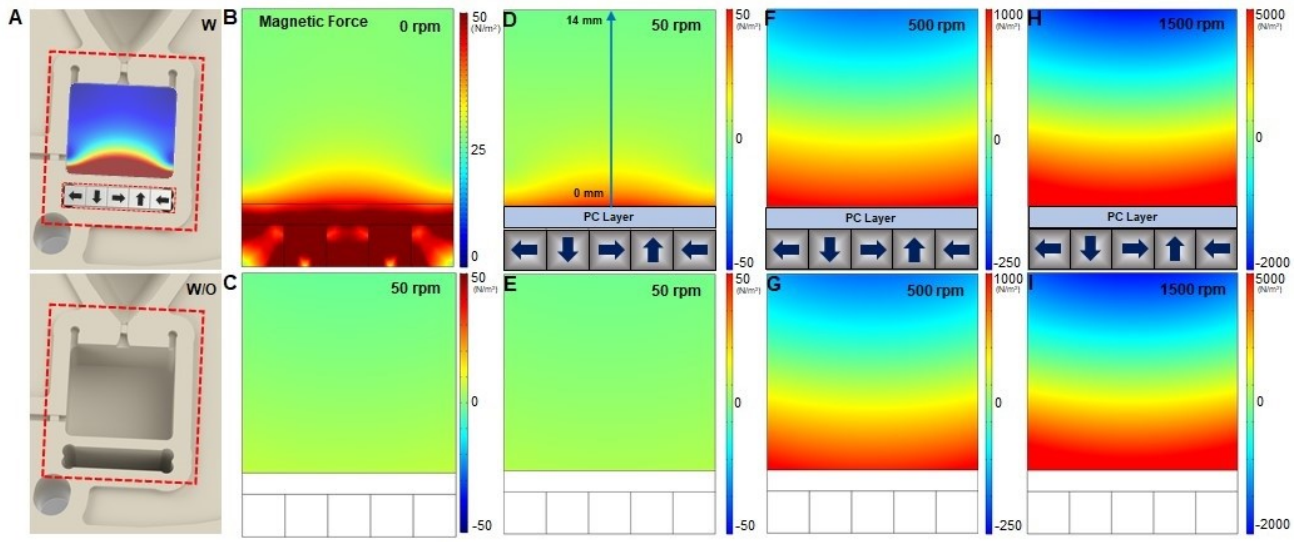

Fig. S2 COMSOL Multiphysics simulation of the total force exerted on the fluid during the purification process with and without the magnets (Halbach array). **(**A**)** Simulation of the existing magnetic force due to the presence (top) and non-existent magnetic force in the absence of the magnets (bottom) beneath the Purification Chamber. (B) Magnetic force exerted on the fluid at 0 RPM. (C and E) Centrifugal force exerted on the fluid at 50 RPM with zero magnetic force. (D) Total force (centrifugal and magnetic) exerted on the fluid at 50 RPM in the presence of the magnets. (F) Total force exerted on the fluid at 500 RPM in the presence of the magnets. (G) Total force exerted on the fluid at 500 RPM in the absence of the magnets. (H) Total force exerted on the fluid at 1,500 RPM with magnets. (I) Total force exerted on the fluid at 1,500 RPM without the magnets.

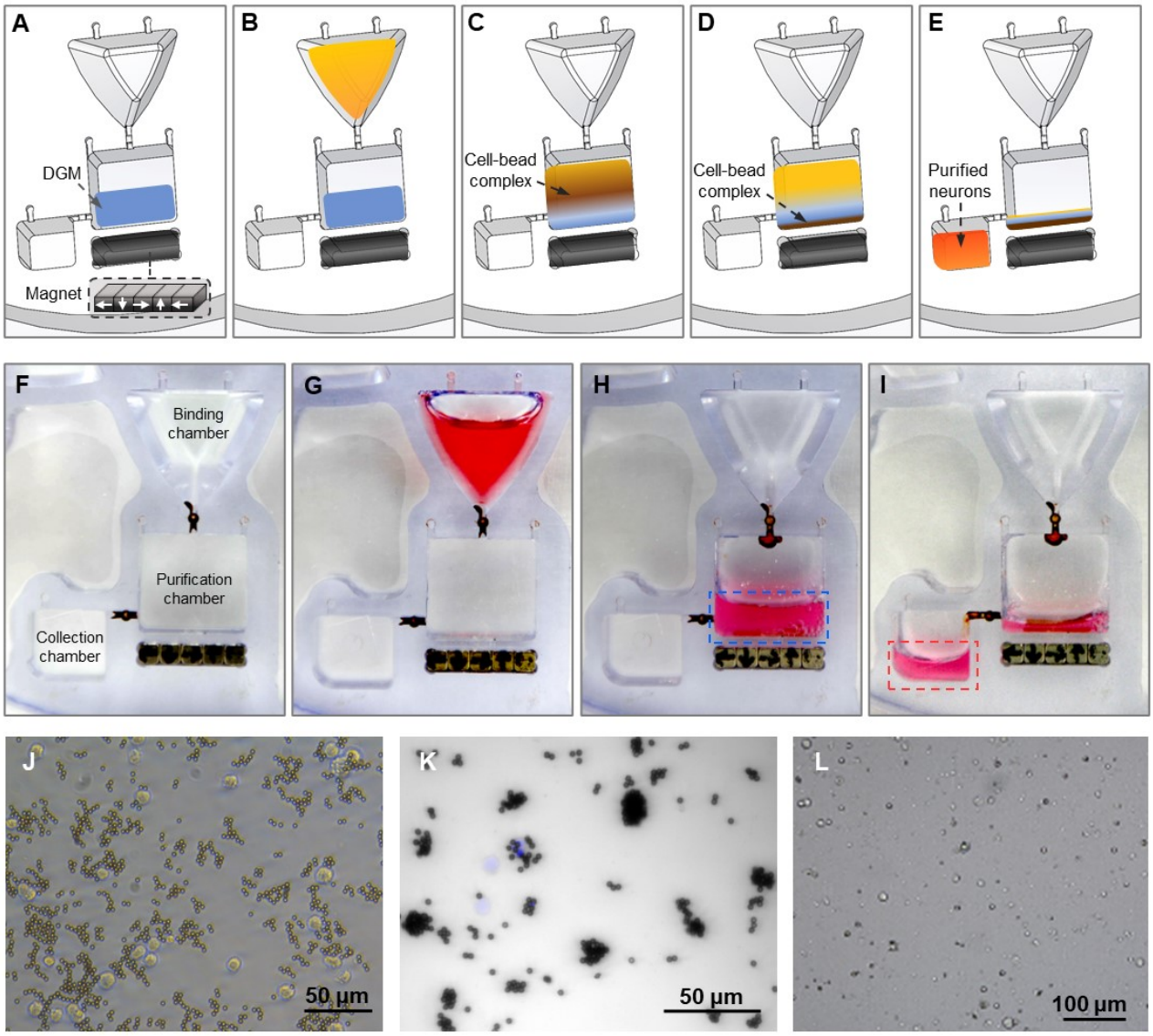

Fig. S3 Neuron purification steps, using the developed CCM-NPD platform. (A-E) Schematic of the DRG neuron purification process using the CCM-NPD platform. (F-I) Images of the actual sequential steps of the CCM-NPD purification. (J-L) Microscopic images of cell suspension (J) after being mixed with immAb in binding chamber, (K) remaining in purification chamber, containing mostly non-neuronal cells-bead complexes and (L) remaining in collection chamber after the completion of the purification, containing mostly purified neurons.

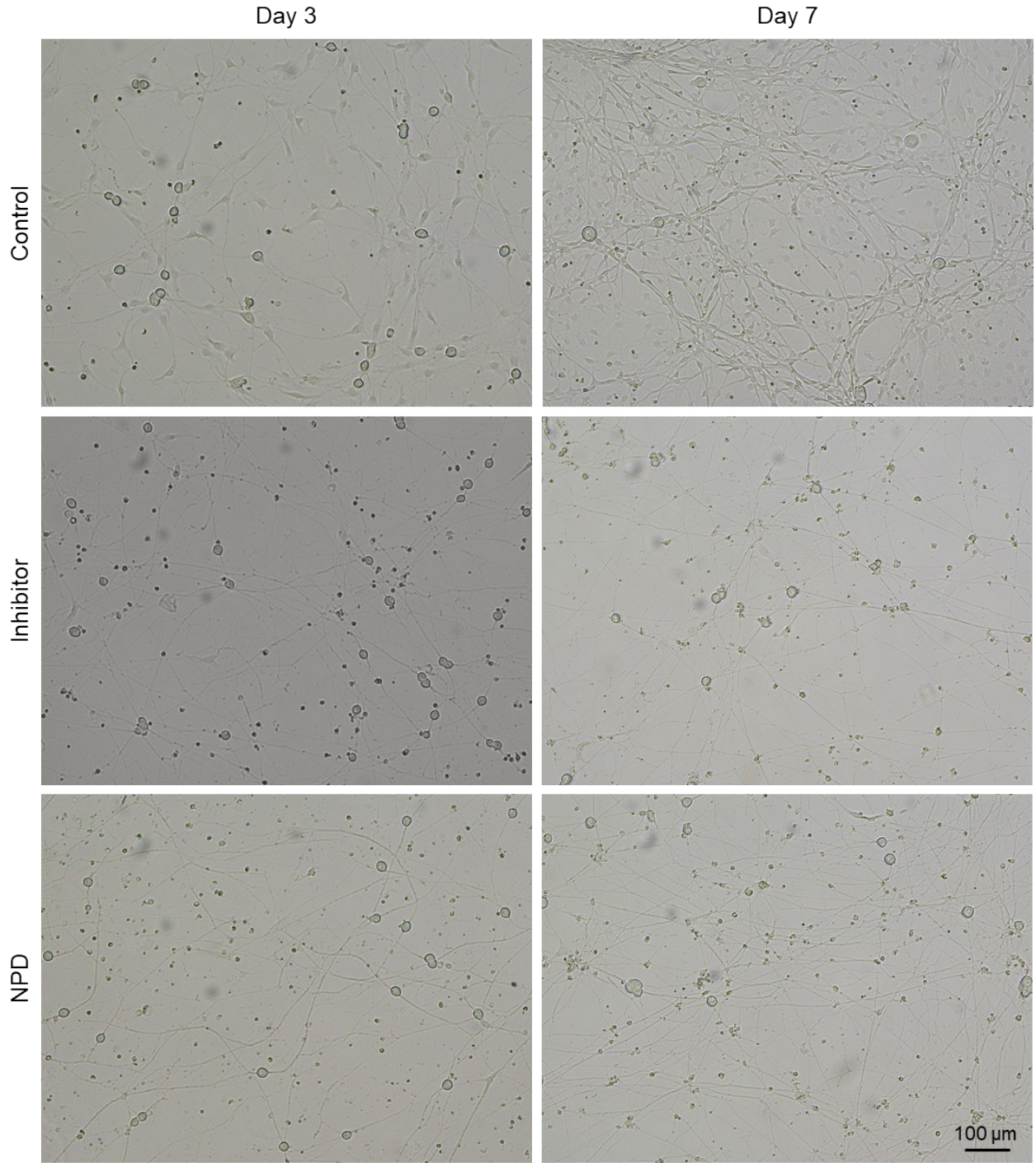

Fig. S4 Bright field images of the non-purified (control), inhibitor-purified and NPD-purified cells on day 3 and day 7 culture.